Prefrontal–hippocampal functional connectivity encodes recognition memory and is impaired in intellectual disability

Maria Alemany-González[a], Thomas Gener[a], Pau Nebot[a], Marta Vilademunt[a], Mara Dierssen[a,b,c,d], and M. Victoria Puig[a,1]

[a]Integrative Pharmacology and Systems Neuroscience, Hospital del Mar Medical Research Institute, Barcelona Biomedical Research Park, 08003 Barcelona, Spain; [b]Cellular and Systems Neurobiology Laboratory, Center for Genomic Regulation, The Barcelona Institute of Science and Technology, 08003 Barcelona, Spain; [c]Cellular and Systems Neurobiology Laboratory, Universitat Pompeu Fabra (UPF), 08003 Barcelona, Spain; and [d]Cellular and Systems Neurobiology Laboratory, Centro de Investigación Biomédica en Red de Enfermedades Raras (CIBERER), 46010 Valencia, Spain

Edited by Ranulfo Romo, National Autonomous University of Mexico, Mexico City, Mexico, and approved April 2, 2020 (received for review December 11, 2019)

Down syndrome (DS) is the most common form of intellectual disability. The cognitive alterations in DS are thought to depend on brain regions critical for learning and memory such as the prefrontal cortex (PFC) and the hippocampus (HPC). Neuroimaging studies suggest that increased brain connectivity correlates with lower intelligence quotients (IQ) in individuals with DS; however, its contribution to cognitive impairment is unresolved. We recorded neural activity in the PFC and HPC of the trisomic Ts65Dn mouse model of DS during quiet wakefulness, natural sleep, and the performance of a memory test. During rest, trisomic mice showed increased theta oscillations and cross-frequency coupling in the PFC and HPC while prefrontal–hippocampal synchronization was strengthened, suggesting hypersynchronous local and cross-regional processing. During sleep, slow waves were reduced, and gamma oscillations amplified in Ts65Dn mice, likely reflecting prolonged light sleep. Moreover, hippocampal sharp-wave ripples were disrupted, which may have further contributed to deficient memory consolidation. Memory performance in euploid mice correlated strongly with functional connectivity measures that indicated a hippocampal control over memory acquisition and retrieval at theta and gamma frequencies, respectively. By contrast, trisomic mice exhibited poor memory abilities and disordered prefrontal–hippocampal functional connectivity. Memory performance and key neurophysiological alterations were rescued after 1 month of chronic administration of a green tea extract containing epigallocatequin-3-gallate (EGCG), which improves executive function in young adults with DS and Ts65Dn mice. Our findings suggest that abnormal prefrontal–hippocampal circuit dynamics are candidate neural mechanisms for memory impairment in DS.

intellectual disability | Down syndrome | learning and memory | functional connectivity | neural networks

Down syndrome (DS, trisomy 21) results from genetic imbalances caused by a triplication of human chromosome 21 (HSA21). DS is characterized by intellectual disability that involves poor learning and memory (1). Animal models of DS have provided insight into plausible cellular and molecular substrates underlying cognitive phenotypes in DS. The Ts65Dn partial trisomic mouse model, where 90 genes orthologous to HSA21 genes are triplicated (2), has provided invaluable insight regarding abnormalities in the cognitive, structural, and cellular domains (3–5). Overall, overexpression of specific HSA21 genes causes dendritic anomalies and disrupted synaptic plasticity in Ts65Dn mice along with excitation–inhibition imbalances that lead to a general overinhibition (6, 7). However, the neurophysiological consequences of these alterations on mesoscopic network connectivity and their impact on cognitive function are poorly understood. Relevant for cognitive performance, DS individuals and Ts65Dn mice suffer from sleep perturbations, including insomnia (8–10). This is important because cortical slow waves and hippocampal ripples during sleep are involved in memory consolidation, and there is a transfer of memories from subcortical to cortical structures (11–13).

Recent neuroimaging studies suggest that brain connectivity is abnormal in individuals with DS, whereby higher regional connectivity correlates with lower intelligence quotients (IQs) (14, 15). This is relevant given that episodic memories depend on a dialogue between the prefrontal cortex (PFC) and the hippocampus (HPC), but it is unclear how such findings directly relate to cognitive dysfunction in DS. Abnormal prefrontal–hippocampal (PFC-HPC) functional connectivity has been postulated as a pathophysiological mechanism for cognitive impairment and sleep disturbances in several brain disorders (16, 17). It is particularly associated with schizophrenia (18, 19) but also contributes to neurodevelopmental and neurodegenerative disorders such as autism, Parkinson's disease, and Alzheimer's disease (20–23).

The present study investigates to what extent functional connectivity disturbances can be linked to memory deficiencies and whether they can be reversed. Although there are currently no therapies for intellectual disability, recent work has demonstrated

Significance

The neural substrates of intellectual disability in Down syndrome (DS, trisomy 21) are still unresolved. We recorded neural activity in brain regions critical for learning and memory, the prefrontal cortex and hippocampus, in the Ts65Dn mouse model of DS during rest, sleep, and memory performance. Trisomic mice exhibited increased local neural activity synchronization and disordered prefrontal–hippocampal functional connectivity during the distinct brain states. Behavioral and selective neurophysiological alterations were rescued by oral administration of a green tea extract containing epigallocatequin-3-gallate (EGCG), which improves executive function in adults with DS and Ts65Dn mice. Our findings suggest that abnormal prefrontal–hippocampal circuit dynamics are candidate neural mechanisms for memory impairment in DS.

Author contributions: M.A.-G., T.G., M.D., and M.V.P. designed research; M.A.-G., T.G., and P.N. performed research; M.A.-G., P.N., M.V., and M.V.P. analyzed data; and M.A.-G., M.D., and M.V.P. wrote the paper.

The authors declare no competing interest.

This article is a PNAS Direct Submission.

Data deposition: Data related to the research discussed in this paper have been deposited in the Mendeley Data repository (https://data.mendeley.com/datasets/wg4zm32gsb/1).

[1]To whom correspondence may be addressed. Email: mpuig3@imim.es.

This article contains supporting information online at https://www.pnas.org/lookup/suppl/doi:10.1073/pnas.1921314117/-/DCSupplemental.

First published May 11, 2020.

that treatment with green tea extracts containing epigallocatechin-3-gallate (EGCG), a flavonoid found in green tea leaves, improves cognitive symptoms in DS. Oral administration of EGCG for several weeks in combination with cognitive training ameliorated recognition memory, inhibitory control, and adaptive behavior in young adults with DS (24). This was accompanied by normalization of increased brain functional connectivity in the frontal, somatosensory, and occipitotemporal cortices and of excessive cortical excitability. EGCG also rescues learning and memory deficits in Ts65Dn mice (25). Here we take advantage of the Ts65Dn DS mouse model to unravel the neurophysiological correlates of memory impairment and the possible mechanisms underlying EGCG-induced memory amelioration. We recorded neural activity simultaneously from the PFC and HPC of Ts65Dn mice and their wild-type nontrisomic littermates during quiet wakefulness and natural sleep. We later investigated neural activity signatures of memory impairment in the novel object recognition task (NOR), which is profoundly impaired in Ts65Dn mice, and examined PFC-HPC network activity recovery after 1 month of oral EGCG.

Results

Ts65Dn Mice Exhibit Prefrontal–Hippocampal Hypersynchronization during Quiet Wakefulness and Sleep. We recorded neural activities in the prelimbic medial PFC and the CA1 region of the HPC of Ts65Dn (TS) mice and their wild-type (WT) littermates (TS

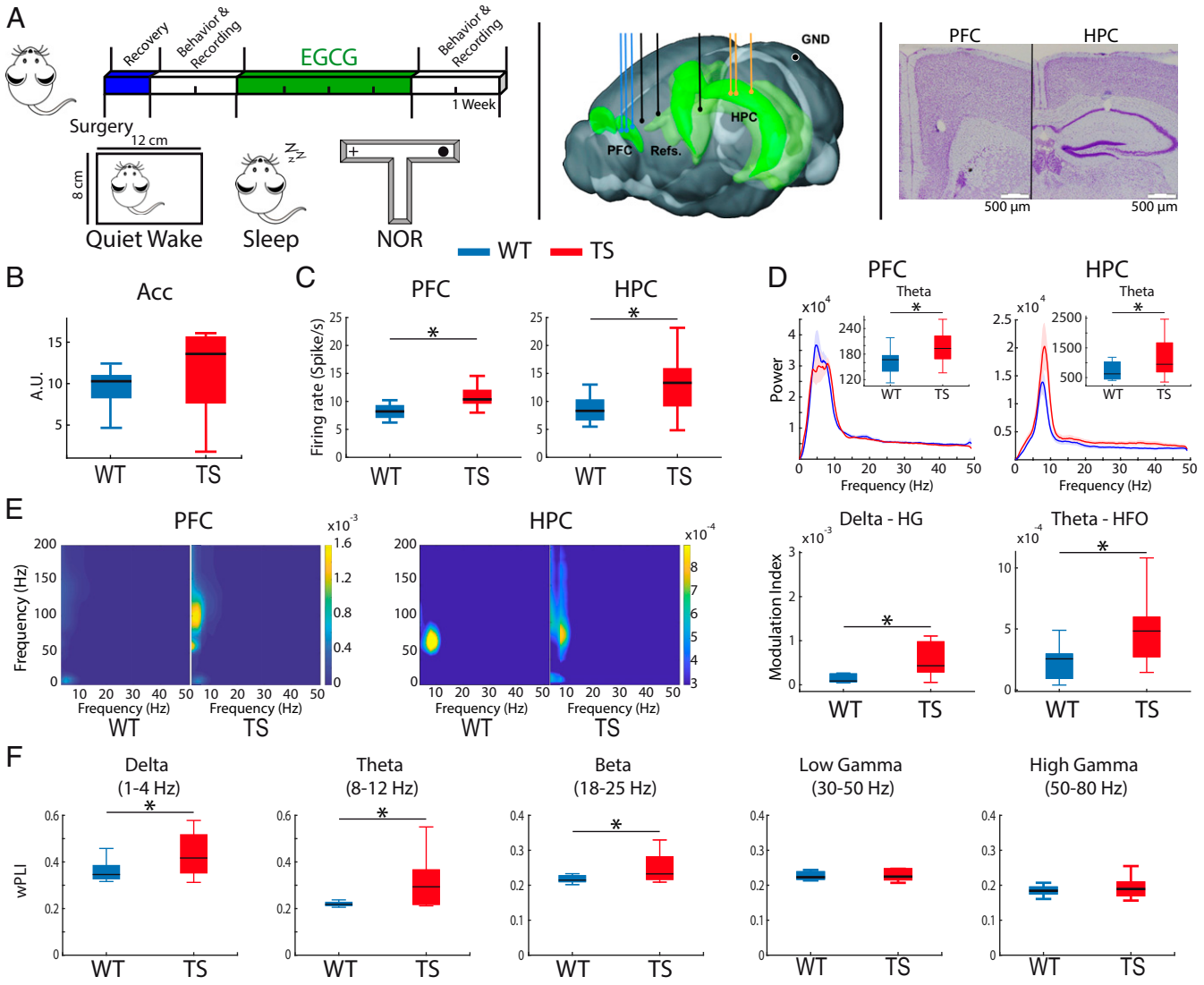

Fig. 1. Ts65Dn mice exhibit prefrontal–hippocampal hypersynchronization during quiet wakefulness. (*A*, *Left*) Experimental timeline and brain states used. Mice were implanted with electrodes in the PFC and HPC at the beginning of the experiment. After a recovery period, behavioral and neurophysiological assessment was carried out during quiet wakefulness, natural sleep, and memory performance in the NOR task. Later, EGCG was administered for 1 month, after which memory performance and neurophysiological activity were investigated again. (*Middle*) Electrode placements within the PFC and HPC and corresponding references (three recording sites each) and ground (GND). (*Right*) Representative example of histological validation. Note the small lesions caused by low-intensity electrical stimulations, which were used to mark the tips of the electrodes after the last recording session in all animals. (*B*) General activity (variance of the acceleration module, Acc) was not different in alert WT ($n = 10$) and Ts65Dn mice ($n = 12$) while animals were in the recording box, where they could move but not walk. (*C*) Mean firing rate of individual neurons in PFC and HPC. (*D*) Power spectra of signals in PFC and HPC. *Insets* depict quantification of theta power. (*E*, *Left*) Comodulation maps of cross-frequency coupling in the PFC and HPC. The color scale indicates the modulation index (MI). (*Right*) Delta (3 to 5 Hz) to high gamma (80 to 120 Hz) MI in PFC and theta to high-frequency oscillation (HFO, 100 to 200 Hz) MI in HPC. Note the different scales between the PFC and HPC. (*F*) Phase synchronization (wPLI) between the PFC and the HPC in both genotypes. The quantification of all neural signals recorded during quiet wakefulness in WT and TS mice is summarized in *SI Appendix*, Table S2. Data are represented as mean ± SEM. *$P \leq 0.05$.

$n = 12$, WT $n = 10$ mice) during quiet wake, natural sleep, and memory performance (Fig. 1*A*). Since TS mice typically display higher locomotion rates than WT mice (26), recordings during quiet wakefulness were performed in a small box that allowed mice to move while locomotion was prevented. In this scenario, the two genotypes showed comparable activity as measured by accelerometer rates (Acc, unpaired *t* test, $P = 0.2$), although the TS group showed more variability (Fig. 1*B*). We found that single-unit firing rates of neurons were increased in TS mice in both areas (PFC: WT 8.6 ± 2 spikes/s, $n = 61$ neurons vs. TS 10.9 ± 2, $n = 65$ neurons, $P = 0.021$; HPC: WT 8.5 ± 2 spikes/s, $n = 50$ neurons vs. TS 13.4 ±5, $n = 56$ neurons, $P = 0.014$) (Fig. 1*C*), from which 60% were putative pyramidal neurons (*SI Appendix*, Fig. S1 and Table S1) (27). TS mice also showed increased power of theta oscillations (8 to 12 Hz) in both structures ($P = 0.04$; Fig. 1*D*). Amplified theta in PFC and HPC did not correlate with animals' activity ($n = 22$ mice; PFC: $R = 0.17$, $P = 0.44$; HPC: $R = 0.25$, $P = 0.24$) and also occurred during resting states when mice explored an open field (*SI Appendix*, Fig. S2), indicating that the increased theta was not simply due to hyperactivity of TS animals or their increased susceptibility to stress when confined in the box. TS mice showed normal power and functional connectivity of other oscillations in both regions (*SI Appendix*, Table S2).

Previous studies have shown that gamma amplitude is strongly modulated by the theta phase (28) and, in fact, hippocampal theta–gamma coupling may be key for associative memory (29). We compared local phase–amplitude cross-frequency coupling between genotypes. TS mice exhibited stronger prefrontal delta to high gamma (3–5 to 80–120 Hz) coupling and hippocampal theta to high frequency (6 to 12 to 100 to 200 Hz) coupling compared to WT mice (unpaired *t* test, $P = 0.04$ and 0.03, respectively) (Fig. 1*E*), suggesting aberrant local hypersynchronization in PFC and HPC. In addition, TS mice displayed increased PFC-HPC long-range functional connectivity (phase synchronization measured via the weighted phase lag index, wPLI) at delta ($P = 0.03$), theta ($P = 0.01$), and beta ($P = 0.03$) frequencies (Fig. 1*F* and *SI Appendix*, Table S2).

We also recorded neural activity during natural sleep following the familiarization phase of the memory task to better capture neural signals related to memory consolidation. Nonrapid eye movement (NREM) sleep was characterized by prominent PFC slow oscillations (<4 Hz) (Fig. 2*A*) and brief HPC high-frequency oscillations (~100 ms, 100 to 250 Hz), referred to as sharp wave ripples. Relevant to this study, cortical slow waves and hippocampal ripples may be critical for offline information processing, including memory consolidation (30). TS mice showed reduced slow oscillations and increased low gamma activity in PFC (WT $n = 9$ vs. TS $n = 11$ mice; unpaired *t* test; $P = 0.03$ and $P = 0.01$, respectively; Fig. 2*B*), whereas no differences were observed in HPC oscillatory activities. Moreover, cross-frequency coupling was normal in TS mice during NREM sleep (*SI Appendix*, Table S2). Furthermore, WT and TS mice exhibited similar occurrences of ripple events (41.7 ± 11.9 and 43.2 ± 9.7 ripples per minute, respectively; $P = 0.63$); however, ripples in TS mice were of lower frequency ($P = 0.03$) and larger amplitude ($P = 0.04$) than in WT mice (Fig. 2*C*). Additionally, PFC-HPC theta phase synchronization (wPLI) was exaggerated in TS mice ($P = 0.034$) (Fig. 2*D*), while no differences were detected at other frequencies (*SI Appendix*, Table S2). Memory processing during sleep can also occur during rapid eye movement (REM) episodes, a faster brain state characterized by prominent theta oscillations in the HPC along with cortical gamma activity (31, 32) (Fig. 2*A*). During REM episodes, PFC theta and beta oscillations were increased in TS mice (WT $n = 8$ vs. TS $n = 11$ mice; Mann–Whitney *U* test, $P = 0.006$ and 0.01), while PFC-HPC synchronization was strengthened at low gamma ranges (unpaired *t* test, $P = 0.009$) (Fig. 2*E*). HPC power was not different across genotypes during REM sleep (*SI Appendix*, Table S2).

Prefrontal–Hippocampal Theta and Gamma Functional Connectivity Contribute to Memory Acquisition, Object Familiarization, and Retrieval in Euploid Mice. We assessed memory abilities with the NOR task, a well-validated memory test in mice that depends on the PFC and HPC (33) and is profoundly impaired in Ts65Dn mice (25, 26, 34–36). The NOR task leverages on the innate motivation of mice to explore novel items in the environment. We used a T-maze adapted for electrophysiological recordings. The task consisted of three sessions of 10 min each: habituation to an empty maze, familiarization of two identical objects placed at the end of the lateral arms, and a memory test 24 h after familiarization when one of the objects was replaced with a novel item (Fig. 3*A*). We recorded electrophysiological activities in the PFC and HPC continuously during the familiarization and memory tests. We first investigated the neural substrates of memory acquisition and object familiarization in the familiarization phase (early vs. late explorations, respectively). We note that memory acquisition cannot be disentangled from novelty seeking; thus, we consider the early visits to the objects the "memory acquisition/novelty" phase and the late visits the "object familiarization" phase. Second, we investigated the neural substrates of "memory retrieval" by comparing neural signals during the visits to the familiar object with those with the novel object during the 24 h test (familiar vs. novel object explorations; Fig. 3*B*). The animals' interactions with the objects were temporally aligned to the electrophysiological recordings by pressing a right or left button on a joystick. This allowed us to investigate the duration and dynamics of object explorations (Fig. 3*C*).

Consistent with the literature (1, 34, 37), WT mice explored more novel objects than familiar objects in the 24 h memory test, and thus, discrimination indexes (DIs) for the novel object were positive (Fig. 3 *D*, *Left*). Positive DIs were not due to differences in the number of explorations of novel and familiar items. Animals performed around 20 to 25 explorations per session (Fig. 3 *D*, *Middle*) with an even number of visits per object (novel vs. familiar object, 14 ± 3 and 11 ± 3, respectively; paired *t* test, $P = 0.11$). Positive DIs resulted from longer explorations of novel than familiar objects ($P = 0.04$; Fig. 3 *D*, *Right*). During the familiarization phase, the total number of exploratory events was also 20 to 25, on average, with similar numbers of visits to the two identical objects (left vs. right object, 14 ± 2 vs. 11 ± 1, $P = 0.2$).

We first aimed to understand the neural mechanisms underlying memory acquisition, object familiarization, and memory retrieval in WT mice. Individual explorations were analyzed in 1 s nonoverlapping windows starting from the button presses, and only windows over 600 ms were included. To investigate memory acquisition and object familiarization, we compared neural activities during the first 5 s with those during the last 5 s of exploration within the familiarization session. For memory retrieval, we examined differences in neural activity between visits to the familiar object and the novel object (all visits included) during the 24 h session. We analyzed local (power), circuit synchronization (wPLI), and the directionality of prefrontal–hippocampal communication (phase slope index, PSI; *SI Appendix*, Table S3).

During the early visits to the objects (memory acquisition/novelty) PFC and HPC theta activities were amplified compared to the late visits ($P = 0.02$; Fig. 3*E* and *SI Appendix*, Table S3). As mice became familiar with the object, PFC-HPC synchronization (wPLI) strengthened at low gamma frequencies ($P = 0.003$). Concurrently, functional connectivity analyses indicated a flow of information from the HPC to the PFC at theta frequencies (HPC to PFC PSI, HPC leads) during the early visits that reversed during the late visits (PFC to HPC PSI, PFC leads; $P = 0.002$; Fig. 3*E*). This is consistent with hippocampal control over object memory acquisition/novelty and prefrontal control over object

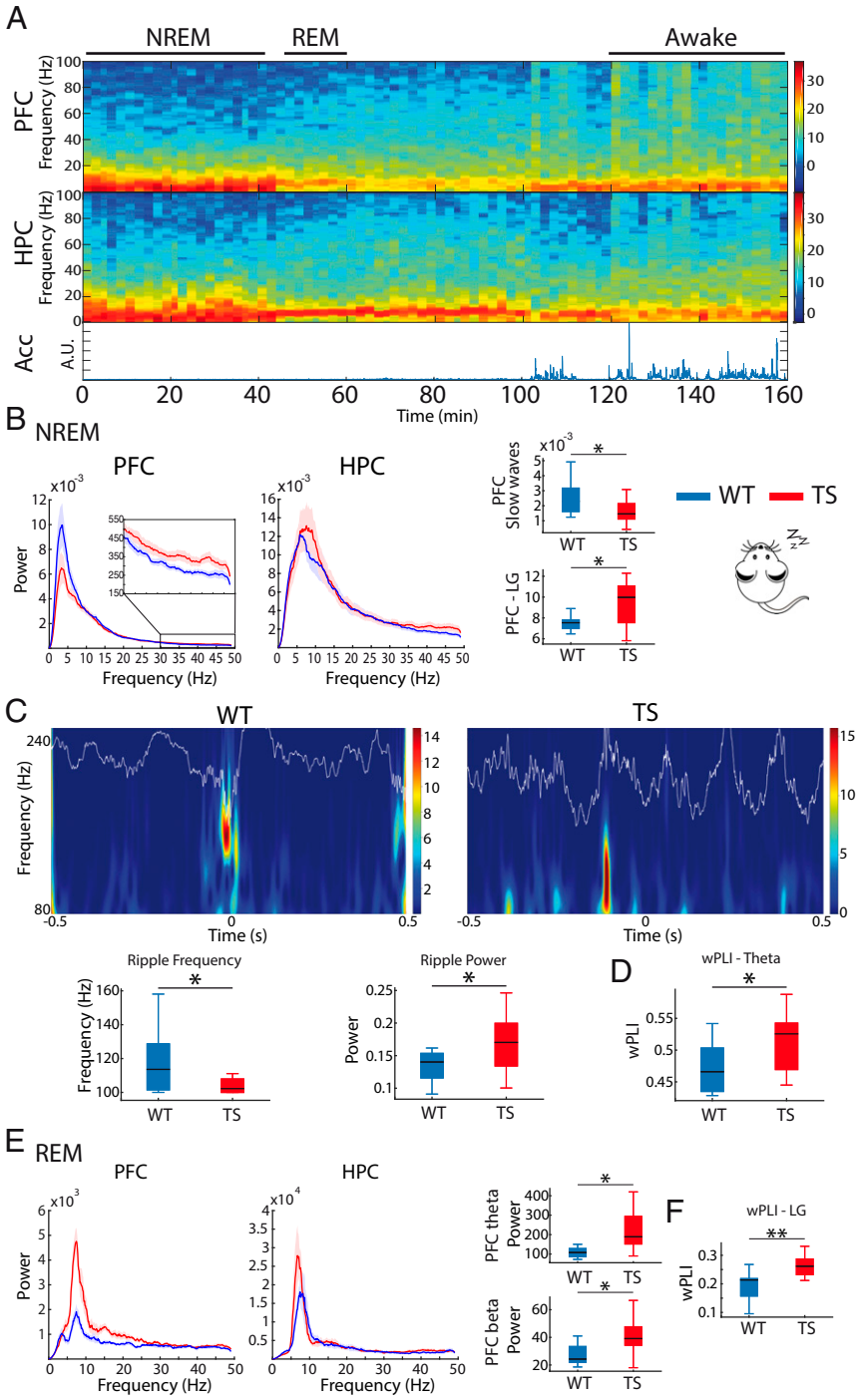

Fig. 2. Ts65Dn mice exhibit prefrontal–hippocampal hypersynchronization during natural sleep. (*A*) Representative spectrograms of neural signals in the PFC and HPC from a WT mouse during wakefulness and REM and NREM sleep. Corresponding general activity (Acc) is shown below. Brain states were classified as awake (large variability of Acc, eyes open), NREM sleep (low variability of Acc, eyes closed, slow waves in PFC), and REM sleep (low variability of Acc, eyes closed, prominent theta oscillations in the HPC, absence of PFC slow waves). (*B*) Power spectra of neural signals in WT and Ts65Dn mice during NREM sleep. *Inset* amplifies spectra at low gamma frequencies (LG, 30 to 50 Hz) in the PFC. Corresponding quantification of slow waves (<4 Hz) and low gamma power in PFC is also shown. (*C*) Wavelet spectrogram of sharp wave ripples recorded in the CA1 area of one WT mouse and one Ts65Dn mouse during NREM sleep. The corresponding LFP traces filtered at ripple frequency (80 to 200 Hz) are superimposed. The quantification of mean ripple frequency and power for each genotype is represented below. (*D*) PFC-HPC phase synchronization (wPLI) at theta frequencies during NREM sleep. (*E*) Power spectra of neural signals in WT and Ts65Dn during REM sleep. Corresponding quantification of theta and beta power in PFC is also shown. (*F*) PFC-HPC phase synchronization (wPLI) at low gamma frequencies during REM sleep. The quantification of all neural signals recorded during sleep in WT and TS mice is summarized in *SI Appendix*, Table S2. Data are represented as mean ± SEM. $*P \leq 0.05$, $**P \leq 0.01$.

familiarization selectively at theta frequencies (Fig. 3*G*). During the 24 h memory test, HPC low gamma power and PFC-HPC high gamma synchronization (wPLI) decreased during the visits to the familiar object ($P = 0.005$ and 0.01, respectively; Fig. 3*F* and *SI Appendix*, Table S3). Furthermore, the direction of information flow traveled from the HPC to the PFC at low gamma

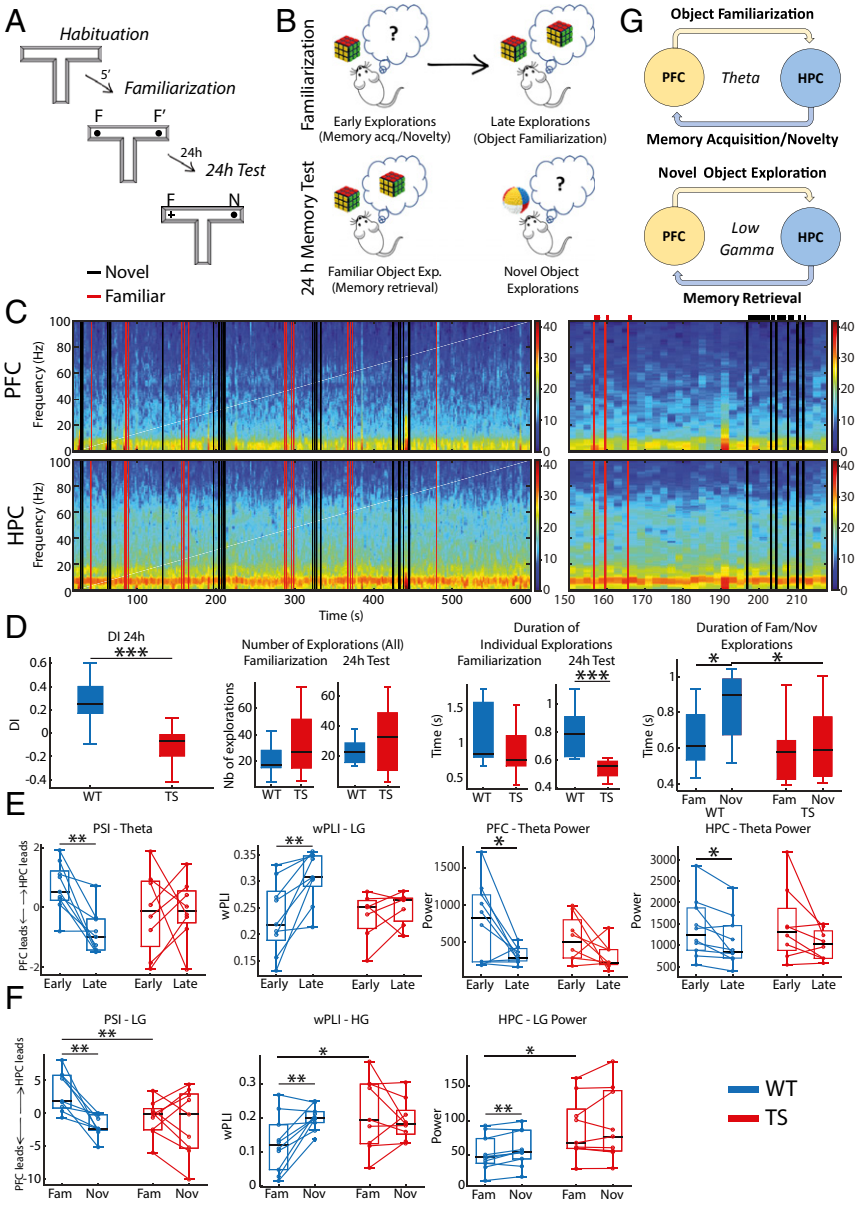

Fig. 3. Neural signals that develop during object familiarization and retrieval in WT mice are disrupted in Ts65Dn mice. (*A*) The novel object recognition task consists of three phases of 10 min each. 1) Habituation phase: Mice first explore an empty maze. 2) Familiarization phase: Mice explore two identical objects placed at the end of the lateral arms of the maze. During this phase memory for the presented object is first acquired and then stored into memory. 3) Twenty-four-hour memory test: Mice explore two objects; one is familiar (presented the previous day), and the other is novel, with the arm chosen randomly in each session. During this phase the memory for the familiar object is retrieved from memory. (*B*) Schematic diagram illustrating memory acquisition and familiarization over multiple explorations of objects during the familiarization phase and memory retrieval when recognizing a familiar object during the 24 h memory test. (*C*) Example spectrogram of a 24 h memory test session of a WT mouse. Black and red lines represent the onset of individual explorations of novel and familiar objects, respectively, detected during the recording session via a video camera and aligned to the electrophysiology system via button presses on a joystick. An amplification of 70 s of the recording is also shown where the duration of each visit is illustrated on top of each line. (*D*) DIs were smaller in Ts65Dn mice compared to their WT littermates during the 24 h memory test. TS mice tended to visit the objects on more occasions than WT mice, during both the familiarization and test phases, but the explorations were shorter, particularly for novel objects in the test phase. Thus, smaller DIs in Ts65Dn mice resulted from shorter explorations of novel objects despite the increased number of visits. (*E*) Neural activities associated with memory acquisition and familiarization. Shown are neural signals recorded during the first 5 s (early) vs. the last 5 s (late) explorations of the two identical objects (ordered in time). In WT mice but not Ts65Dn mice, PFC to HPC theta connectivity and PFC-HPC low gamma phase synchronization strengthened as items were stored into memory (late visits). By contrast, theta power in PFC and HPC decreased. (*F*) Neural activities associated with memory retrieval. Shown are neural signals recorded during all explorations of the familiar and novel objects in one session. In WT mice but not Ts65Dn mice, HPC to PFC low gamma connectivity strengthens as items are retrieved from memory. This is accompanied by weakening of PFC-HPC high gamma phase synchronization and HPC low gamma power. (*G*) Proposed contribution of PFC-HPC circuits to memory acquisition, familiarization, and retrieval in the NOR task in WT mice. The quantification of all neural signals recorded during the NOR task in WT and TS mice is summarized in *SI Appendix*, Tables S3 and S4. $^{*}P \leq 0.05$, $^{**}P \leq 0.01$, $^{***}P \leq 0.001$.

frequencies (HPC to PFC PSI, HPC leads) that reversed when mice explored the novel object, consistent with hippocampal control over object memory retrieval at low gamma (Fig. 3*F*). Altogether, functional connectivity measures suggested that neural signals in the PFC and the HPC coordinate at theta and low gamma frequencies during memory acquisition and retrieval, respectively, with the HPC playing a leading role (Fig. 3*G*). These connectivity fluctuations were frequency specific and did not occur at other frequencies (*SI Appendix*, Table S3).

Ts65Dn Mice Exhibit Poor Object Recognition Memory and Abnormal Prefrontal–Hippocampal Neurodynamics. Discrimination indexes were smaller in TS mice with respect to WT mice (WT $n = 10$ vs. TS $n = 11$ mice; unpaired t test; $P < 0.00005$) (Fig. 3 *D*, *Left*), an indication of poor recognition memory. Again, the smaller DIs were not due to differences in the number of explorations but in their duration. Although the mean number of explorations per session was slightly higher than in WT mice (Fig. 3 *D*, *Middle*), TS mice explored novel and familiar objects evenly (15.2 ± 3.6 vs. 18.2 ± 4.1 times, respectively; paired t test, $P = 0.31$). Noteworthily, the duration of individual explorations was shorter than in WT mice (unpaired t test, $P < 0.00005$), particularly for novel objects ($P = 0.04$). Consequently, visits to novel and familiar objects lasted equally in TS mice (paired t test, $P = 0.63$) (Fig. 3 *D*, *Right*). A repeated measures ANOVA with duration of novel and familiar explorations as within factor and genotype as between factor showed a significant novelty × genotype interaction ($F_{1,18} = 5{,}38$; $P = 0.032$), indicating that the relative duration of novel and familiar explorations was unequal across genotypes. Smaller DIs could also result from behavioral differences during the familiarization phase. During familiarization, TS mice made more visits to the objects than WT mice (TS = 33.5 ± 7.2 vs. WT = 20.8 ± 3.75, $P = 0.14$), but these were shorter (TS = 0.54 ± 0.02 vs. WT = 0.8 ± 0.05 s, $P = 0.0004$). Importantly, the total exploration time was comparable across genotypes (TS = 18.6 ± 3.37 vs. WT = 20.17 ± 4.55 s, $P = 0.79$); thus, both groups of mice had similar time to acquire information about the objects.

The neurophysiological signatures associated with memory acquisition, object familiarization, and memory retrieval in WT mice were abnormal in TS mice (Fig. 3 *E* and *F* and *SI Appendix*, Table S4). HPC to PFC theta directionality (PSI) and PFC-HPC low gamma synchronization (wPLI) were not different during early and late explorations (paired t test, $P = 0.92$ and 0.4, respectively). An ANOVA with time (early or late explorations) as within factor and genotype as between factor showed a significant time × genotype interaction for both measures ($F_{1,15} = 5.11$, $P = 0.03$; $F_{1,14} = 6{,}08$, $P = 0.02$, respectively), indicating that early to late transitions were different across genotypes. In addition, PFC and HPC theta oscillations were not amplified during early visits (paired t test, $P = 0.13$ and 0.11, respectively; Fig. 3*E*). During the 24 h memory test, HPC to PFC low gamma directionality (PSI), PFC-HPC high gamma synchronization (wPLI), and HPC low gamma power were not different when exploring familiar and novel objects ($P = 0.67$, 0.48, and 0.34, respectively) (Fig. 3*F*). Accordingly, an ANOVA showed a significant time × genotype interaction for the three parameters ($F_{1,16} = 5.11$, $P = 0.04$; $F_{1,16} = 6.34$, $P = 0.023$; $F_{1,17} = 7{,}81$, $P = 0.012$), revealing that familiar vs. novel interactions were different across genotypes. We further detected exaggerated wPLI and HPC power at gamma in TS mice compared to WT mice during visits to familiar objects (WT $n = 10$ vs. TS $n = 9$ mice; unpaired t test, $P = 0.04$ and 0.05, respectively).

We further examined whether increased neuroinflammatory response to craniotomies or abnormal myelination in TS mice could explain the neurophysiological differences from WT mice. We quantified microglia and myelin (via Iba1+ and MBP+ immunostaining, respectively) and found no differences across genotypes (*SI Appendix*, Figs. S3 and S4).

Chronic Oral EGCG Rescues Memory Impairment in Ts65Dn Mice and Partially Normalizes Prefrontal–Hippocampal Abnormal Neurodynamics. We used the procognitive compound EGCG to validate the neural signatures of memory impairment identified above. EGCG is a flavonoid found in green tea leaves that ameliorates executive function in individuals with Down syndrome and in mouse models (25, 38). TS mice were administered EGCG in their drinking water for 1 month following procedures reported previously (25), and neural activity was later recorded as in pre-EGCG epochs (Fig. 1*A*). Two TS animals that only received water served as controls (black dots in Fig. 4). EGCG rescued memory abilities in TS mice (DIs before vs. after EGCG, TS $n = 8$ mice; paired t test, $P = 0.02$; Fig. 4*A*). We classified TS mice as responders and nonresponders based on the change of DI (DI post-EGCG − DI pre-EGCG) and found that six TS mice (the responders) showed robust increases of DI (+0.5 ± 0.21), indicating better memory after EGCG. The two other animals performed more poorly after EGCG (−0.12 and −0.18) and were classified as nonresponders (orange dots in Fig. 4). Responder mice extended the duration of their explorations, particularly the visits to novel objects that were now longer than to familiar objects (pre- vs. post-EGCG; $P = 0.02$ and 0.024, respectively; Fig. 4*A*). These behavioral changes remained in the EGCG-treated group even when including the nonresponders (DI: $P = 0.02$; time of explorations: $P = 0.02$). When comparing WT baseline and TS post-EGCG to determine the possible rescue of the trisomic phenotype to WT levels, an ANOVA with duration of novel and familiar explorations as within factor and genotype as between factor did not show a significant novelty × genotype interaction ($F_{1,12} = 1.31$, $P = 0.27$) but a significant effect of novelty ($F_{1,12} = 8.89$, $P = 0.01$), indicating different duration of novel and familiar visits in both genotypes.

In addition, EGCG normalized several neural activities in TS mice across brain states. During quiet wakefulness EGCG reduced excessive power of PFC theta oscillations to WT levels only in responder mice (theta power before vs. after EGCG in six responder mice; paired t test, $P = 0.03$; theta power in seven WT mice during baseline vs. six EGCG-treated responder mice, unpaired t test, $P = 0.9$) (Fig. 4*B*). However, during NREM sleep the power of ripple events was corrected in all treated mice (seven TS mice [one responder mouse lost the implant]; paired t test, $P = 0.04$; five responder mice, $P = 0.04$; seven WT mice during baseline vs. seven EGCG-treated TS mice, unpaired t test, $P = 0.43$) (Fig. 4*C*). EGCG also normalized some neural activities associated with memory acquisition, object familiarization, and memory retrieval (*SI Appendix*, Table S4). EGCG rescued theta power fluctuations during the familiarization phase in the PFC and HPC (theta power during early vs. late visits in PFC and HPC; all TS $n = 7$ vs. WT $n = 10$ mice during baseline, ANOVA $F_{1,15} = 17.91$ and 37.03, $P = 0.001$ and 0.0005, respectively; 5 responder TS vs. 10 WT mice, $F_{1,13} = 15.02$ and 26.48, $P = 0.002$ and 0.0005, respectively). Also, a consistent HPC to PFC flow of information at theta emerged during the early visits as in WT mice (all treated vs. WT mice; ANOVA $F_{1,14} = 25.73$, $P = 0.0005$; responders vs. WT mice, $F_{1,12} = 36.53$, $P = 0.0004$) (Fig. 4*D*). Moreover, EGCG rescued the main PFC-HPC connectivity alterations detected during the memory test (disordered PSI low gamma and PLI high gamma during familiar vs. novel visits; all treated mice vs. WT mice; ANOVA $F_{1,14} = 33.79$ and 12.51, $P = 0.0005$ and 0.003, respectively; responders vs. WT mice, $F_{1,12} = 26.13$ and 21.08, $P = 0.0005$ and 0.001, respectively) (*SI Appendix*, Table S4). We note that EGCG corrected some neural activities in the two nonresponder mice, an effect not observed in the two controls with water (orange vs. black dots in Fig. 4).

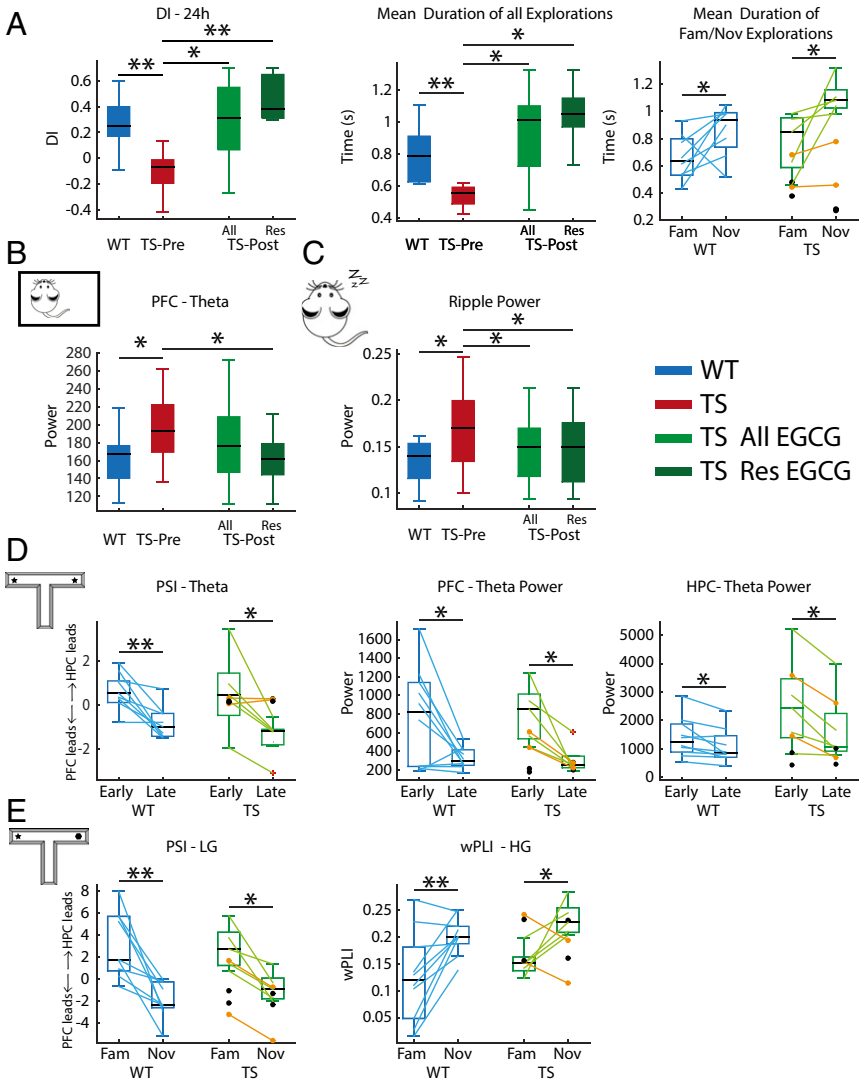

Fig. 4. Chronic oral EGCG rescues memory impairment and corrects several prefrontal–hippocampal disordered neurodynamics in Ts65Dn mice. (*A*) EGCG increased DIs in six (Res, responders only) of eight (All, responders and nonresponders) treated TS mice. In all panels, orange dots correspond to the two EGCG nonresponders, whereas black dots represent the two TS control mice that only received water. Corresponding measures obtained during the baseline period in WT mice are shown for reference. DIs were normalized in TS mice because individual explorations were longer, particularly when visiting novel objects. (*B*) EGCG reduced amplified PFC theta oscillations in responder mice to WT levels during quiet wakefulness. (*C*) EGCG reduced amplified ripple power in all treated mice to WT levels during NREM sleep. (*D*) During the familiarization phase, EGCG promoted a consistent PFC to HPC flow at theta in TS mice and proper decreases of theta power in PFC and HPC during the late visits to objects. (*E*) During the 24 h test, EGCG promoted a correct HPC to PFC flow at low gamma (LG) in TS mice during memory retrieval. In addition, PFC-HPC high gamma (HG) phase synchronization was rescued. The effects of EGCG on all neural signals recorded in TS mice across brain states are summarized in *SI Appendix*, Tables S2 and S4. $*P \leq 0.05$, $**P \leq 0.01$.

We also investigated the temporal effects of EGCG by assessing memory abilities in TS mice 1 month after the treatment had subsided. TS mice performed worse after EGCG had washed out (DIs of five TS mice during baseline, EGCG, and washout; ANOVA $F_{2,6} = 16.21$, $P = 0.004$) (*SI Appendix*, Fig. S6), pointing to transient effects of EGCG. Finally, because TS mice may regulate body temperature more poorly that WT mice (39), we examined whether an effect of EGCG on temperature regulation could explain the behavioral and neurophysiological rescue. We found that body temperature regulation was similar across genotypes before, during, and after a 10 d treatment with EGCG ($F_{1,4} = 0.41$, $P = 0.55$) (*SI Appendix*, Fig. S6).

Prefrontal–Hippocampal Neurodynamics Predict Memory Performance in Euploid and Ts65Dn Mice. The results presented above raised the possibility of an association between PFC-HPC disordered neurodynamics and deficient memory in Ts65Dn mice. To investigate this further, we examined correlations between neural activities and memory performance (DIs in the 24 h memory test) in WT and TS mice. We found that the power of PFC theta oscillations during quiet wakefulness correlated negatively with DIs when including both genotypes (Pearson's correlation; $n = 20$ mice, 10 WT and 10 TS; $R = -0.61$; $P = 0.004$). That is, large-amplitude theta oscillations predicted poor memory performance. Notably, DIs showed strong dependence on PFC theta power in TS mice but not in WT mice (WT: $R = -0.28$, $P = 0.43$; TS: $R = -0.69$, $P = 0.02$). This PFC theta dependence subsided with EGCG in the five responders ($R = 0.25$, $P = 0.62$), but not when the two nonresponders were included (all treated: $R = -0.64$, $P = 0.08$) (Fig. 5*A*).

Furthermore, PFC to HPC theta connectivity (PSI) present during the late visits to objects correlated negatively with DIs in WT mice ($R = -0.78$; $P = 0.01$), underscoring that a flow of

information from PFC to HPC at theta frequencies may be necessary for proper object familiarization. In TS mice this relationship only emerged after EGCG treatment (eight treated TS mice; baseline: $R = 0.22$, $P = 0.58$; EGCG: $R = -0.85$, $P = 0.01$) (Fig. 5*B*). Conversely, HPC to PFC low gamma PSI during familiar object explorations in the memory test correlated positively with memory performance ($R = 0.7$, $P = 0.036$), with those animals with robust HPC to PFC low gamma PSI being the best performers. Again, in TS mice this association only started to emerge after EGCG (baseline: $R = 0.11$, $P = 0.76$; EGCG: $R = 0.69$, $P = 0.08$) (Fig. 5*B*). Other abnormal neural activities detected during memory acquisition, familiarization, and retrieval did not correlate with memory performance.

Multiple regression analyses provided further support to the significance of these correlations. Multiple regression models predicted DIs with high accuracy when combining PFC theta power during rest, PFC-HPC theta directionality (PSI) during object familiarization, and PFC-HPC low gamma directionality (PSI) during memory retrieval in WT mice ($F_{3,4} = 27.44$, $P = 0.004$, $R^2 = 0.95$). All three variables contributed significantly to the prediction (*SI Appendix*, Table S5). By contrast, they were not able to predict memory performance in TS mice ($F_{3,4} = 0.082$, $P = 0.96$, $R^2 = 0.052$), with marginal contribution of the three variables. In the five responder TS mice multiple regression models predicted post-EGCG DIs with high accuracy ($F_{3,4} = 1809$, $P = 0.01$, $R^2 = 1$).

Discussion

In this study we demonstrate that Ts65Dn mice, a well-established model of DS, exhibit hypersynchronized neural activity in prefrontal–hippocampal circuits during distinct brain states, including quiet wakefulness, sleep, and memory performance. TS mice also show disordered PFC-HPC communication during memory acquisition, object familiarization, and retrieval. Some of these abnormal neural activities could contribute to intellectual disability in DS as they correlate strongly with memory impairment. This is also supported by the fact that chronic EGCG ameliorates memory performance and normalizes these neural activities.

During quiet wakefulness, spiking activity and theta power in the PFC and HPC were increased in TS mice. Cortical theta oscillations are associated with working memory and cognitive flexibility (40–42) and are augmented in adults with DS (43). These large prefrontal theta oscillations predicted poor memory performance in TS mice and were reduced by EGCG. Thus, amplified prefrontal theta in DS may be pathological and reflect cortical hypersynchronization of neural networks in resting states. Excessive theta was not an artifact of animal motion since we took care to mitigate the effects of hyperlocomotion of TS animals and strong theta–DI correlations persisted even though they were measured on different days. Hippocampal theta oscillations are also involved in several cognitive processes such as spatial and memory processing (44), but they did not correlate with memory performance in either genotype.

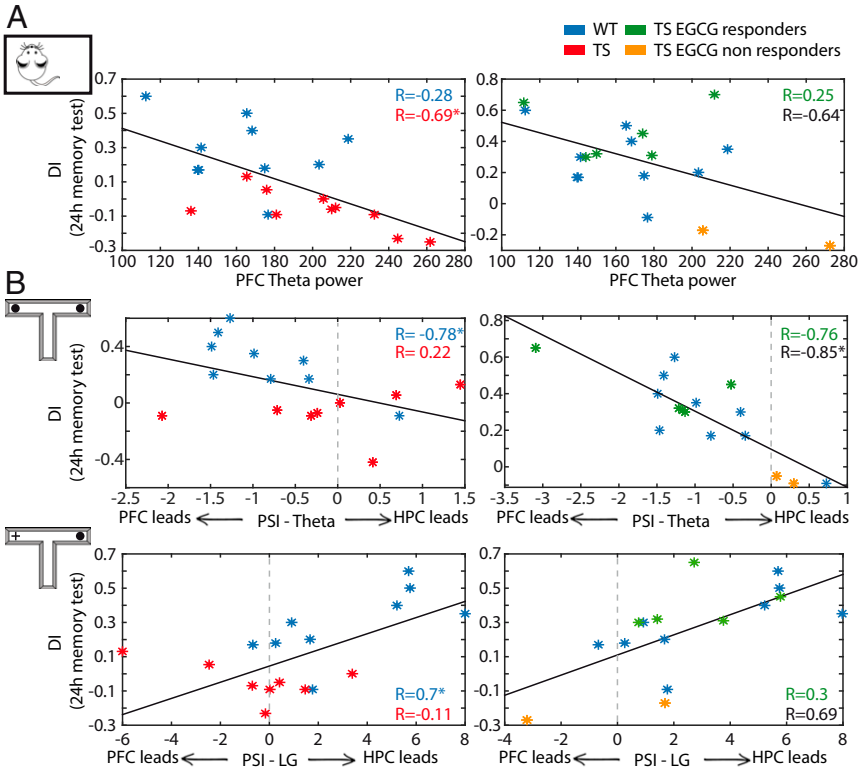

Fig. 5. Key prefrontal–hippocampal neurophysiological biomarkers predict memory performance. (*A*) PFC theta power recorded during quiet wakefulness correlated with DIs assessed during the 24 h memory test (on a different day) in Ts65Dn mice (red asterisks and correlation coefficient); i.e., large-amplitude theta oscillations predicted poor memory performance. This dependence subsided after EGCG in the six EGCG responders (green asterisks and correlation coefficient) and in one of the two nonresponders (orange). Correlation coefficients of all EGCG-treated TS mice are shown in black. Corresponding measures for WT mice (blue asterisks and correlation coefficient) obtained during baseline periods are shown for reference. In WT mice PFC theta power did not correlate with DIs. (*B*) PFC to HPC theta PSI that emerged during the late visits to objects correlated negatively with DIs in WT mice; i.e., animals with more consistent PFC to HPC theta communication performed better. This relationship only emerged in the five responding TS mice after EGCG (note the distinct scales for both the DIs and the PSIs between the two plots). During the 24 h test, HPC to PFC low gamma PSI correlated positively with DIs in WT mice; i.e., animals with more consistent HPC to PFC low gamma performed better. This relationship only emerged in the five responding TS mice after EGCG. $^*P \leq 0.05$.

Cross-frequency coupling was also stronger in TS mice in both structures, another sign of excessive neural synchronization. Hippocampal theta–gamma coupling has been linked to associative memory (29), and cortical theta–gamma coupling is enhanced in a mouse model of epilepsy that concurs with memory impairment (45). Therefore, excessive cortical coupling in TS mice is consistent with the increased prevalence of epilepsy in DS (46). TS mice also exhibited increased PFC-HPC theta phase synchronization, as if the PFC-HPC circuit was locked to theta oscillatory regimes with increased local theta power and cross-regional theta synchronization. Appropriate PFC-HPC synchrony is key for diverse behavioral and cognitive functions, and its disruption contributes to psychiatric and neurological disorders. Our results are consistent with increased synchrony of brain networks in DS subjects that inversely correlates with intelligence quotients (IQ) (14, 15).

This hypersynchronization was also observed in TS mice during natural sleep. During REM sleep, the "wake like" sleep, PFC theta oscillations were amplified in TS mice as in quiet alertness. Frontal EEG theta is increased in Ts65Dn mice during REM sleep, which is associated with sleep disturbances (8) similar to those observed in DS subjects (9). During NREM sleep, cortical slow waves were shallower in TS mice while low gamma oscillations were amplified, further reflecting prolonged episodes of light sleep. In addition, NREM PFC-HPC theta phase synchronization was augmented compared to WTs, in concordance with previous EEG studies (43). Our observations of increased cortical activity and cross-regional synchronization during sleep in Ts65Dn mice may explain insomnia in DS, as recently suggested by studies in human subjects (47). We also recorded HPC sharp-wave ripples after the familiarization phase to capture events relevant for memory consolidation (48). We hypothesized that abnormal ripples could contribute to memory impairment in Ts65Dn mice as observed in Dp16 trisomic mice (49). Ripples were remarkably slow and enlarged in TS mice. EGCG normalized ripple amplitude, providing further evidence that ripple alterations may have contributed to poor memory performance by preventing a correct consolidation of familiar objects into memory.

Elevated spiking rates of pyramidal neurons in Ts65Dn mice may have been reflected in larger theta and gamma oscillations in the PFC and HPC (32). Increased excitability of pyramidal neurons has been associated with premature aging in Ts65Dn mice (50, 51), as these mice show early-onset Alzheimer's disease after 6 months of age. Here we discard premature aging as a main factor because the quantification of firing rates was performed in 3-month-old TS mice. In addition, excessive G protein-coupled inward-rectifying potassium channels (GIRK2) in Ts65Dn mice could also result in the pathological theta reported here (52, 53).

DS individuals show deficits in declarative memory that could arise from deficient memory consolidation and also from poor memory acquisition, retrieval, and learning abilities (54). In Ts65Dn mice declarative memory is also faulty, as revealed by poor spatial navigation and recognition memory (1, 5, 34, 35, 37). Here the DIs of TS mice were smaller than those of WT mice because individual explorations were shorter, despite TS mice tending to visit the objects on more occasions, possibly reflecting hyperlocomotion and attentional deficits (26, 54, 55). After EGCG, visits to novel objects were as long as in WT mice; thus, TS mice showed the ability to discriminate between new and familiar items for the first time. This indicates that EGCG ameliorated memory processing, but we cannot exclude a beneficial effect on attention.

We further explored neural activities of PFC-HPC circuits as candidate cellular mechanisms for memory acquisition, familiarization, and retrieval. A robust consensus exists on the key role of the HPC in recognition memory based on previous damage and lesion studies in humans and monkeys (56), while a contribution of the PFC is also acknowledged (57). Our study strongly suggests the participation of both structures in memory acquisition, familiarization, and retrieval and points to PFC-HPC cross-regional communication as a key element. More specifically, two complementary neural mechanisms may be involved. Memory acquisition depends on HPC to PFC flow of information at theta frequencies that switches direction as objects become familiar. Memory retrieval also depends on HPC to PFC flow of information but at low gamma frequencies. The fact that TS mice exhibited disordered information flow during poor memory performance that was rescued by EGCG provides further support for this hypothesis. Moreover, our findings strongly imply that TS mice show faulty neural mechanisms for memory acquisition, familiarization, and retrieval.

Chronic treatment with EGCG alleviates DS symptoms and improves cognitive performance both in DS subjects and Ts65Dn mice (24, 25). Moreover, EGCG normalizes excessive intracortical facilitation in DS subjects, suggesting that it might improve cognitive abilities via the normalization of an overexcited cerebral cortex (24). Here EGCG normalizes pathological theta activity across brain states (quiet wake, sleep, and memory performance), amplified sleep ripples, and PFC-HPC directionality associated with memory impairment in Ts65Dn mice. The procognitive effects of EGCG have not been fully elucidated, but it likely has multiple mechanisms of action. EGCG exerts broad effects on several nonneuronal targets, including myelination (57) and microbiota (58). Several studies have demonstrated that EGCG crosses the blood–brain barrier in rodents after oral administration (59–61), including in TgDyrk1A transgenic mice, another genetic model of Down syndrome (62). In fact, EGCG has been detected in rat frontal cortex and hippocampus (60), so the effects observed in our study could be, indeed, mediated by direct action of EGCG on these structures. Recently, Gu et al. demonstrated that EGCG inhibits DYRK1A activity in TgDyrk1A transgenic mice (62), a kinase encoded by the triplicated Dyrk1A gene that has been associated with multiple cognitive functions (63, 64). Since the exact mechanisms of action of EGCG may involve multiple targets, it is plausible that it affects behavior through mechanisms beyond oscillatory synchrony. Multiple linear regression analyses allowed the investigation of the relationships between memory performance and neural activities and revealed that a combination of PFC theta activity during rest, PFC to HPC theta PSI, and HPC to PFC low gamma PSI during memory performance accounted for 95% of the variance in the discrimination indices. Remarkably, these three measures, which were recorded on three separate days, were normalized by EGCG.

In closing, we identified neural signatures of disrupted PFC-HPC circuits in Ts65Dn mice across distinct brain states that may be relevant for understanding sleep disturbances and memory impairment in DS. Selective neural activities associated with memory processing were corrected by EGCG, suggesting that EGCG may be a promising treatment for cognitive symptoms in DS. Our results may help elucidate the neural substrates of intellectual disability and sleep disturbances in DS and other cognitive disorders, shedding light onto the understanding of these pathologies and the development of novel therapeutic strategies.

Summary of Methods

The full methods can be found in the *SI Appendix*.

Animals. Ts65Dn male mice (TS, $n = 12$) and their wild-type littermates (WT, $n = 10$) were obtained by breeding B6EiC4Sn.BLiA-Ts(1716)65Dn/DnJ females with C57BL/6 × 6JOlaHsd (B6C3F1/OlaHsd) hybrid males. Mice were genotyped, and ∼25% of the offspring presented trisomy. Mice were housed on a conventional 12:12 light cycle, and behavioral testing and recordings were conducted during the light phase. All procedures had authorization from the Barcelona Biomedical Research Park Animal Research Ethics Committee

(PRBB-CEEA) and the local government (Generalitat de Catalunya) and were conducted according to the European Directive 2010/63/EU and Spanish regulations RD 53/2013.

Experimental Design. Mice were implanted with microelectrodes at 2 to 3 months of age. After a postsurgical recovery period, neural activity was recorded during several brain states (quiet wakefulness, REM and NREM sleep, recognition memory). Then, EGCG (Life Extension, 45%, 2 to 3 mg per day) was administered for 1 month in the drinking water. Afterward, a behavioral and neurophysiological characterization was performed as in pre-EGCG epochs. Finally, mice were killed, and electrode placements were confirmed histologically (Fig. 1*A*).

Behavioral and Neurophysiological Characterization. Three tungsten electrodes (25 μm) were implanted in the prelimbic medial PFC, and three more were implanted in the CA1 area of the HPC. We recorded single-unit activity (SUA) and local field potentials (LFPs) with the Open Ephys system with a sampling rate of 30 kHz. We used the accelerometer's signals to monitor general mobility of mice (65). SUA was estimated by referencing the signal, filtering between 450 and 6,000 Hz and sorting the spikes with Offline Sorter. To obtain LFPs, signals were down-sampled to 1 kHz, detrended, and notch filtered with custom-written scripts in Python. Signals were then imported into MATLAB. The frequency bands considered for the band-specific analyses included delta (1 to 4 Hz), theta (8 to 12 Hz), beta (18 to 25 Hz), low gamma (30 to 50 Hz), and high gamma (50 to 80 Hz).

Quiet wakefulness and NREM and REM sleep. Recordings during quiet wakefulness were performed in a small box that allowed mice to move but not to walk. Recordings during natural sleep were implemented following the familiarization phase of the NOR task to capture neural signals related to memory consolidation. NREM sleep was defined as animal immobility (low variations of the accelerometer) and large-amplitude slow oscillations (1 to 4 Hz) in the PFC and HPC. REM sleep epochs were defined as animal immobility and prominent hippocampal theta rhythms (Fig. 2*A*). Analyses of LFPs signals during quiet wakefulness and natural sleep were performed by averaging neural signals over one continuous epoch per experiment (quiet wakefulness: 3 min; NREM sleep: 1 min; REM sleep: 10 s).

The novel object recognition task. We tested recognition memory using a well-established task that relies on the innate instinct of mice to explore novel objects in the environment (66). The test was implemented in three phases of 10 min each: habituation, familiarization, and memory test 24 h after familiarization. During familiarization, mice could explore two identical objects located at the end of the two lateral arms. During the test phase, mice were presented with one familiar and one novel object. Object recognition memory was defined by the discrimination index (DI) for the novel object: DI = [novel object exploration time − familiar object exploration time]/total exploration time (64). Memory acquisition was investigated during the familiarization phase. We ordered the explorations of the two objects in time and compared neural activity during the first 5 s and the last 5 s of exploration (in 1 s windows). Memory retrieval was investigated during the 24 h memory test by comparing neural signals during explorations of familiar versus novel objects.

Data and Statistical Analyses. All analyses were carried out with custom scripts programmed in Python (data preprocessing, Acc) and MATLAB (power, cross-frequency modulation index, ripples, wPLI, PSI). A summary of all of the functions used with links to the original sources can be found in the *SI Appendix*. The complete dataset with statistical results can be found in the *SI Appendix*. All data are represented as the mean ± SEM. We used paired and unpaired *t* tests and repeated measures ANOVAs to compare measures across genotypes and to assess the effects of EGCG. To identify significant correlations between LFP measures and DIs, Pearson and Spearman correlations were used for parametric and nonparametric distributions, respectively. Multiple regression models were used to estimate the relative contribution of LFP measures to memory performance.

All quantified data files have been deposited in the Mendeley Data repository (https://data.mendeley.com/datasets/wg4zm32gsb/1).

ACKNOWLEDGMENTS. We thank R. de la Torre, P. Robledo, E. Kossatz, O. Valverde, C. Delgado, and P. Calvé for helpful comments on this article. We also thank M. Valero for providing the script to analyze hippocampal ripples and A. Tauste-Campo for providing the script to analyze wPLI. This work was supported by the Ministerio de Ciencia, Innovación y Universidades together with the Fondo Europeo de Desarrollo Regional (Grants #AEI-SAF2013-49129-C2-2-R and #AEI-SAF2016-80726-R to M.V.P., #AEI-SAF2016-79956-R to M.D.), Generalitat de Catalunya (#2017-SGR-210 to M.V.P. and #2017-SGR-926 to M.D.) and by the Jerome Lejeune Foundation (to M.V.P.). This work was also supported by the Horizon 2020 GO-DS21 grant, the Fundació La Marató De TV3 (Grant 201620-31 to M.D.), the European Commission JPND HEROES grant, and the National Institutes of Health (Grant NIH-1R01EB 028159-01) to M.D. The CIBER of Rare Diseases is an initiative of the Instituto de Salud Carlos III (ISCIII). We also acknowledge the support of the Spanish Ministry of Science and Innovation to the EMBL partnership, the Centro de Excelencia Severo Ochoa and the CERCA Programme/Generalitat de Catalunya. M.V.P. was supported by the Ramon y Cajal Investigator Program (Award RyC-2012-10042), and M.A.-G. was supported by a FPI predoctoral fellowship (Award BES-2014-070429).

1. M. Dierssen, Down syndrome: The brain in trisomic mode. *Nat. Rev. Neurosci.* **13**, 844–858 (2012).
2. M. Gupta, A. R. Dhanasekaran, K. J. Gardiner, Mouse models of Down syndrome: Gene content and consequences. *Mamm. Genome* **27**, 538–555 (2016).
3. M. Dierssen *et al*., Alterations of neocortical pyramidal cell phenotype in the Ts65Dn mouse model of Down syndrome: Effects of environmental enrichment. *Cereb. Cortex* **13**, 758–764 (2003).
4. M. T. Davisson *et al*., Segmental trisomy as a mouse model for Down syndrome. *Prog. Clin. Biol. Res.* **384**, 117–133 (1993).
5. R. H. Reeves *et al*., A mouse model for Down syndrome exhibits learning and behaviour deficits. *Nat. Genet.* **11**, 177–184 (1995).
6. A. M. Kleschevnikov *et al*., Hippocampal long-term potentiation suppressed by increased inhibition in the Ts65Dn mouse, a genetic model of Down syndrome. *J. Neurosci.* **24**, 8153–8160 (2004).
7. P. V. Belichenko, A. M. Kleschevnikov, A. Salehi, C. J. Epstein, W. C. Mobley, Synaptic and cognitive abnormalities in mouse models of Down syndrome: Exploring genotype-phenotype relationships. *J. Comp. Neurol.* **504**, 329–345 (2007).
8. D. Colas *et al*., Sleep and EEG features in genetic models of Down syndrome. *Neurobiol. Dis.* **30**, 1–7 (2008).
9. L. C. Nisbet, N. N. Phillips, T. F. Hoban, L. M. O'Brien, Characterization of a sleep architectural phenotype in children with Down syndrome. *Sleep Breath.* **19**, 1065–1071 (2015).
10. H. C. Heller, N. F. Ruby, Functional interactions between sleep and circadian rhythms in learning and learning disabilities. *Handb. Exp. Pharmacol.* **253**, 425–440 (2019).
11. C. M. Wierzynski, E. V. Lubenov, M. Gu, A. G. Siapas, State-dependent spike-timing relationships between hippocampal and prefrontal circuits during sleep. *Neuron* **61**, 587–596 (2009).
12. S. Diekelmann, J. Born, The memory function of sleep. *Nat. Rev. Neurosci.* **11**, 114–126 (2010).
13. B. O. Watson, G. Buzsáki, Sleep, memory & brain rhythms. *Daedalus* **144**, 67–82 (2015).
14. J. S. Anderson *et al*., Abnormal brain synchrony in Down syndrome. *Neuroimage Clin.* **2**, 703–715 (2013).
15. J. Pujol *et al*., Anomalous brain functional connectivity contributing to poor adaptive behavior in Down syndrome. *Cortex* **64**, 148–156 (2015).
16. M. Li, C. Long, L. Yang, Hippocampal-prefrontal circuit and disrupted functional connectivity in psychiatric and neurodegenerative disorders. *BioMed Res. Int.* **2015**, 810548 (2015).
17. M. V. Puig, T. Gener, Serotonin modulation of prefronto-hippocampal rhythms in health and disease. *ACS Chem. Neurosci.* **6**, 1017–1025 (2015).
18. T. Sigurdsson, S. Duvarci, Hippocampal-prefrontal interactions in cognition, behavior and psychiatric disease. *Front. Syst. Neurosci.* **9**, 190 (2016).
19. T. Sigurdsson, K. L. Stark, M. Karayiorgou, J. A. Gogos, J. A. Gordon, Impaired hippocampal-prefrontal synchrony in a genetic mouse model of schizophrenia. *Nature* **464**, 763–767 (2010).
20. L. Wang *et al*., Changes in hippocampal connectivity in the early stages of Alzheimer's disease: Evidence from resting state fMRI. *Neuroimage* **31**, 496–504 (2006).
21. P. J. Uhlhaas, W. Singer, Neural synchrony in brain disorders: Relevance for cognitive dysfunctions and pathophysiology. *Neuron* **52**, 155–168 (2006).
22. P. J. Uhlhaas, W. Singer, Abnormal neural oscillations and synchrony in schizophrenia. *Nat. Rev. Neurosci.* **11**, 100–113 (2010).
23. W. Pettersson-Yeo, P. Allen, S. Benetti, P. McGuire, A. Mechelli, Dysconnectivity in schizophrenia: Where are we now? *Neurosci. Biobehav. Rev.* **35**, 1110–1124 (2011).
24. R. de la Torre *et al*.; TESDAD study group, Safety and efficacy of cognitive training plus epigallocatechin-3-gallate in young adults with Down's syndrome (TESDAD): A double-blind, randomised, placebo-controlled, phase 2 trial. *Lancet Neurol.* **15**, 801–810 (2016).
25. R. De la Torre *et al*., Epigallocatechin-3-gallate, a DYRK1A inhibitor, rescues cognitive deficits in Down syndrome mouse models and in humans. *Mol. Nutr. Food Res.* **58**, 278–288 (2014).
26. M. Faizi *et al*., Comprehensive behavioral phenotyping of Ts65Dn mouse model of Down syndrome: Activation of β1-adrenergic receptor by xamoterol as a potential cognitive enhancer. *Neurobiol. Dis.* **43**, 397–413 (2011).
27. H. Kim, S. Ährlund-Richter, X. Wang, K. Deisseroth, M. Carlén, Prefrontal parvalbumin neurons in control of attention. *Cell* **164**, 208–218 (2016).
28. E. Nyhus, T. Curran, Functional role of gamma and theta oscillations in episodic memory. *Neurosci. Biobehav. Rev.* **34**, 1023–1035 (2010).

29. A. B. L. Tort, R. W. Komorowski, J. R. Manns, N. J. Kopell, H. Eichenbaum, Theta-gamma coupling increases during the learning of item-context associations. *Proc. Natl. Acad. Sci. U.S.A.* **106**, 20942–20947 (2009).
30. G. Buzsáki, Hippocampal sharp wave-ripple: A cognitive biomarker for episodic memory and planning. *Hippocampus* **25**, 1073–1188 (2015).
31. R. Boyce, S. D. Glasgow, S. Williams, A. Adamantidis, Causal evidence for the role of REM sleep theta rhythm in contextual memory consolidation. *Science* **352**, 812–816 (2016).
32. G. Buzsáki, Theta oscillations in the hippocampus. *Neuron* **33**, 325–340 (2002).
33. E. C. Warburton, M. W. Brown, Neural circuitry for rat recognition memory. *Behav. Brain Res.* **285**, 131–139 (2015).
34. F. Fernandez, C. C. Garner, Episodic-like memory in Ts65Dn, a mouse model of Down syndrome. *Behav. Brain Res.* **188**, 233–237 (2008).
35. F. Fernandez *et al*., Pharmacotherapy for cognitive impairment in a mouse model of Down syndrome. *Nat. Neurosci.* **10**, 411–413 (2007).
36. J. Braudeau *et al*., Chronic treatment with a promnesiant GABA-A α5-selective inverse agonist increases immediate early genes expression during memory processing in mice and rectifies their expression levels in a Down syndrome mouse model. *Adv. Pharmacol. Sci.* **2011**, 153218 (2011).
37. A. Navarro-Romero *et al*., Cannabinoid type-1 receptor blockade restores neurological phenotypes in two models for Down syndrome. *Neurobiol. Dis.* **125**, 92–106 (2019).
38. F. Guedj *et al*., Green tea polyphenols rescue of brain defects induced by overexpression of DYRK1A. *PLoS One* **4**, e4606 (2009).
39. M. R. Stasko, A. C. S. Costa, Experimental parameters affecting the Morris water maze performance of a mouse model of Down syndrome. *Behav. Brain Res.* **154**, 1–17 (2004).
40. K. Benchenane *et al*., Coherent theta oscillations and reorganization of spike timing in the hippocampal- prefrontal network upon learning. *Neuron* **66**, 921–936 (2010).
41. H. Lee, G. V. Simpson, N. K. Logothetis, G. Rainer, Phase locking of single neuron activity to theta oscillations during working memory in monkey extrastriate visual cortex. *Neuron* **45**, 147–156 (2005).
42. P.-K. O'Neill, J. A. Gordon, T. Sigurdsson, Theta oscillations in the medial prefrontal cortex are modulated by spatial working memory and synchronize with the hippocampus through its ventral subregion. *J. Neurosci.* **33**, 14211–14224 (2013).
43. S. Hamburg, R. Rosch, C. M. Startin, K. J. Friston, A. Strydom, Dynamic causal modeling of the relationship between cognition and theta-alpha oscillations in adults with Down syndrome. *Cereb. Cortex* **29**, 2279–2290 (2019).
44. T. Korotkova *et al*., Reconciling the different faces of hippocampal theta: The role of theta oscillations in cognitive, emotional and innate behaviors. *Neurosci. Biobehav. Rev.* **85**, 65–80 (2018).
45. A. Maheshwari *et al*., Persistent aberrant cortical phase-amplitude coupling following seizure treatment in absence epilepsy models. *J. Physiol.* **595**, 7249–7260 (2017).
46. R. W. McVicker, O. E. P. Shanks, R. J. McClelland, Prevalence and associated features of epilepsy in adults with Down's syndrome. *Br. J. Psychiatry* **164**, 528–532 (1994).
47. J. Leerssen *et al*., Increased hippocampal-prefrontal functional connectivity in insomnia. *Neurobiol. Learn. Mem.* **160**, 144–150 (2019).
48. G. Buzsáki, Hippocampal sharp waves: Their origin and significance. *Brain Res.* **398**, 242–252 (1986).
49. M. Raveau *et al*., Alterations of in vivo CA1 network activity in Dp(16)1Yey Down syndrome model mice. *eLife* **7**, e31543 (2018).
50. T. K. Best, M. Cho-Clark, R. J. Siarey, Z. Galdzicki, Speeding of miniature excitatory post-synaptic currents in Ts65Dn cultured hippocampal neurons. *Neurosci. Lett.* **438**, 356–361 (2008).
51. F. Stagni *et al*., Long-term effect of neonatal inhibition of APP gamma-secretase on hippocampal development in the Ts65Dn mouse model of Down syndrome. *Neurobiol. Dis.* **103**, 11–23 (2017).
52. S. J. Kang *et al*., Family-based genome-wide association study of frontal θ oscillations identifies potassium channel gene KCNJ6. *Genes Brain Behav.* **11**, 712–719 (2012).
53. T. K. Best, N. P. Cramer, L. Chakrabarti, T. F. Haydar, Z. Galdzicki, Dysfunctional hippocampal inhibition in the Ts65Dn mouse model of Down syndrome. *Exp. Neurol.* **233**, 749–757 (2012).
54. S. Vicari, S. Bellucci, G. A. Carlesimo, Implicit and explicit memory: A functional dissociation in persons with Down syndrome. *Neuropsychologia* **38**, 240–251 (2000).
55. H. C. Heller *et al*., Nest building is impaired in the Ts65Dn mouse model of Down syndrome and rescued by blocking 5HT2a receptors. *Neurobiol. Learn. Mem.* **116**, 162–171 (2014).
56. L. R. Squire, J. T. Wixted, R. E. Clark, Recognition memory and the medial temporal lobe: A new perspective. *Nat. Rev. Neurosci.* **8**, 872–883 (2007).
57. M. Lepage, M. Brodeur, P. Bourgouin, Prefrontal cortex contribution to associative recognition memory in humans: An event-related functional magnetic resonance imaging study. *Neurosci. Lett.* **346**, 73–76 (2003).
58. U. Gundimeda *et al*., Polyphenols from green tea prevent antineuritogenic action of Nogo-A via 67-kDa laminin receptor and hydrogen peroxide. *J. Neurochem.* **132**, 70–84 (2015).
59. K. Nakagawa, T. Miyazawa, Absorption and distribution of tea catechin, (-)-epigallocatechin-3-gallate, in the rat. *J. Nutr. Sci. Vitaminol. (Tokyo)* **43**, 679–684 (1997).
60. L. C. Lin, M. N. Wang, T. Y. Tseng, J. S. Sung, T. H. Tsai, Pharmacokinetics of (-)-epigallocatechin-3-gallate in conscious and freely moving rats and its brain regional distribution. *J. Agric. Food Chem.* **55**, 1517–1524 (2007).
61. B.-B. Wei, M.-Y. Liu, X. Zhong, W.-F. Yao, M.-J. Wei, Increased BBB permeability contributes to EGCG-caused cognitive function improvement in natural aging rats: Pharmacokinetic and distribution analyses. *Acta Pharmacol. Sin.* **40**, 1490–1500 (2019).
62. Y. Gu *et al*., Molecular rescue of Dyrk1A overexpression alterations in mice with Fontup® dietary supplement: Role of green tea catechins. *Int. J. Mol. Sci.* **21**, 1404 (2020).
63. A. Duchon, Y. Herault, DYRK1A, a dosage-sensitive gene involved in neurodevelopmental disorders, is a target for drug development in Down syndrome. *Front. Behav. Neurosci.* **10**, 104 (2016).
64. S. García-Cerro *et al*., Overexpression of Dyrk1A is implicated in several cognitive, electrophysiological and neuromorphological alterations found in a mouse model of Down syndrome. *PLoS One* **9**, e106572 (2014).
65. T. Gener *et al*., Serotonin 5-HT_{1A}, 5-HT_{2A} and dopamine D_2 receptors strongly influence prefronto-hippocampal neural networks in alert mice: Contribution to the actions of risperidone. *Neuropharmacology* **158**, 107743 (2019).
66. M. Leger *et al*., Object recognition test in mice. *Nat. Protoc.* **8**, 2531–2537 (2013).